SANDIA REPORT
SAND2011-0173
Unlimited Release
Printed January 2011

Self-Activating and Doped Tantalate Phosphors

May D. Nyman and Lauren E. S. Rohwer

Prepared by
Sandia National Laboratories
Albuquerque, New Mexico 87185 and Livermore, California 94550

Sandia National Laboratories is a multi-program laboratory managed and operated by Sandia Corporation, a wholly owned subsidiary of Lockheed Martin Corporation, for the U.S. Department of Energy's National Nuclear Security Administration under contract DE-AC04-94AL85000.

Approved for public release; further dissemination unlimited.

Issued by Sandia National Laboratories, operated for the United States Department of Energy by Sandia Corporation.

NOTICE: This report was prepared as an account of work sponsored by an agency of the United States Government. Neither the United States Government, nor any agency thereof, nor any of their employees, nor any of their contractors, subcontractors, or their employees, make any warranty, express or implied, or assume any legal liability or responsibility for the accuracy, completeness, or usefulness of any information, apparatus, product, or process disclosed, or represent that its use would not infringe privately owned rights. Reference herein to any specific commercial product, process, or service by trade name, trademark, manufacturer, or otherwise, does not necessarily constitute or imply its endorsement, recommendation, or favoring by the United States Government, any agency thereof, or any of their contractors or subcontractors. The views and opinions expressed herein do not necessarily state or reflect those of the United States Government, any agency thereof, or any of their contractors.

Printed in the United States of America. This report has been reproduced directly from the best available copy.

Available to DOE and DOE contractors from
U.S. Department of Energy
Office of Scientific and Technical Information
P.O. Box 62
Oak Ridge, TN 37831

Telephone: (865) 576-8401
Facsimile: (865) 576-5728
E-Mail: reports@adonis.osti.gov
Online ordering: http://www.osti.gov/bridge

Available to the public from
U.S. Department of Commerce
National Technical Information Service
5285 Port Royal Rd.
Springfield, VA 22161

Telephone: (800) 553-6847
Facsimile: (703) 605-6900
E-Mail: orders@ntis.fedworld.gov
Online order: http://www.ntis.gov/help/ordermethods.asp?loc=7-4-0#online

SAND2011-0173
Unlimited Release
Printed January 2011

Self-Activating and Doped Tantalate Phosphors

May D. Nyman
Geochemistry Department

Lauren E. S. Rohwer
Advanced Microsystems Packaging Department

Sandia National Laboratories
P.O. Box 5800
Albuquerque, New Mexico 87185-MS0745

Abstract

An ideal red phosphor for blue LEDs is one of the biggest challenges for the solid-state lighting industry. The appropriate phosphor material should have good adsorption and emission properties, good thermal and chemical stability, minimal thermal quenching, high quantum yield, and is preferably inexpensive and easy to fabricate. Tantalates possess many of these criteria, and lithium lanthanum tantalate materials warrant thorough investigation. In this study, we investigated red luminescence of two lithium lanthanum tantalates via three mechanisms: 1) Eu-doping, 2) Mn-doping and 3) self-activation of the tantalum polyhedra. Of these three mechanisms, Mn-doping proved to be the most promising. These materials exhibit two very broad adsorption peaks; one in the UV and one in the blue region of the spectrum; both can be exploited in LED applications. Furthermore, Mn-doping can be accomplished in two ways; ion-exchange and direct solid-state synthesis. One of the two lithium lanthanum tantalate phases investigated proved to be a superior host for Mn-luminescence, suggesting the crystal chemistry of the host lattice is important.

ACKNOWLEDGMENTS

This work was funded by the Sandia National Laboratories LDRD program. We thank Dr. Hongwu Xu of LANL for the Neutron Diffraction study of La_2LiTaO_6.

CONTENTS

FIGURES

TABLES

NOMENCLATURE

DTA	Differential thermal analysis
Eu	Europium
La	Lanthanum
LED	light emitting diode
Li	Lithium
Mn	Manganese
QY	quantum yield
Ta	Tantalum
TGA	Thermogravimetric Analysis

1. INTRODUCTION

Luminescent materials, or phosphors, are useful in numerous applications including imaging, detection, tagging, decoration, and lighting. They are in forms of thin films, monoliths, or powders for miscellaneous devices, or dispersible nanoparticles for applications such as biomedical imaging. We are particularly interested in oxide phosphors (as apposed to chalcogenides or pnictides) due to their inherent chemical and thermal stability and minimal toxicity to the biosphere. Tantalates are very promising materials for these applications because they are especially robust and resistant to chemical degradation. Furthermore, studies have shown that rare-earth tantalates are excellent host lattices for Eu-doped red-emitting phosphors, excited by blue light.(**1-4**) The specific application we have explored is phosphors for improved color rendering of blue LEDs for solid-state lighting. Discovery of an ideally suitable red phosphor for this application could potentially revolutionize this highly-competitive, advanced high technology industry.

In this ~9 month LDRD project, we have explored the use of lithium lanthanum tantalate materials for blue-excitation, red-emitting phosphors for solid-state lighting. These oxide host lattices, $Li_5La_3Ta_2O_{12}$ and $LiTaLa_2O_6$ are well-known solid-state electrolytes for lithium conductivity (**5-8**), yet they have not been investigated for phosphor applications. They potentially offer great flexibility in that the lattice can accommodate substitutions and vacancies. These variations provide opportunity to optimize the luminescence characteristics such as by shifting and broadening adsorption and emission peaks, and increasing the quantum yield, or brightness of emission. For red-emission, we have explored 1) Eu-doping, 2) Mn-doping and 3) self-activation. We are particularly interested in the latter two, in that there will potentially be limited availability of rare-earths in the near future due to political strategies of China, the major international exporter of rare-earths compounds.

2. RESULTS AND DISCUSSION

2.1 Description of Structures and Dopant Strategies

The first lithium lanthanum tantalate of interest, $Li_5La_3Ta_2O_{12}$, has cubic garnet structure, and will be denoted LiLaTa-garnet in this discussion; refer to **figure 1** for a view of the lattice structure. The Ta-site is octahedral with Ta-O bond distances of 2.0 Å on average. There are several Li-sites; and the exact geometries and occupancies of these sites is variable, depending on processing conditions. The lithium in these sites are very mobile, thus the materials have known ion –conductivity behavior. **Figure 1** emphasizes the channels of connected Li-sites along which the Li-ions can travel through the lattice. Lithium coordination in LiLaTa-garnet is either tetrahedral or octahedral. Li-O bond lengths in the tetrahedral sites are ~1.8 Å, and ~2.0 Å in the octahedral site. There is also likely some substitution of Li on the Ta-site, since Li and Ta have the exact same metal-oxygen bond length in octahedral coordination. Furthermore, the high mobility of the Li renders site-to-site hopping in the framework. The La is 8-coordinate with bond lengths varying from 2.4-2.6 Å, a perfect site for substitution of Eu. Finally, we hoped to observe self-activating luminescence of Ta-polyhedra. This is well-known for oxide lattices containing tetrahedral NbO_4, such as $LaNbO_4$: a blue emission is observed under UV-excitation. (**9**) However, isostructural $LaTaO_4$ does not have a strong emission, due to the fact that it is octahedral, not tetrahedral. In the LiLaTa-garnet, oxygen vacancies can be created via Li_2O volatilization upon prolonged heating. Therefore self-activated tantalate luminescence might be observed as a result of oxygen defects and the resultant low coordination of Ta.

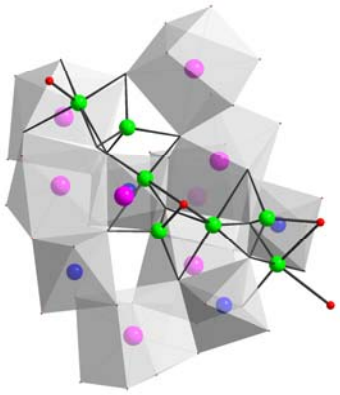

Figure 1.
LiLaTa-garnet. Blue is octahedral Ta, pink is 8-coordinate La(Eu), green is tetrahedral and octahedral Li.

The second lithium lanthanum tantalate of interest is La_2LiTaO_6, which has the perovskite structure, denoted LiLaTa-perovskite. This phase, based on its powder diffraction pattern first reported in 1986 (**11**) was presumed to be isostructural with several other compounds including La_2IrZnO_6 and La_2IrNiO_6,(**12**) but the structure had not been refined. Therefore we have determined the structure using a combination of neutron scattering and X-ray diffraction data (see experimental). The two methods were utilized in order to optimize signal from both Li

(neutron scattering) and the heavier metals (X-ray diffraction). The structure parameters and atomic positions (for data collected at 300 K) are summarized in **Table 1**. The observed, calculated and difference spectra for the neutron scattering data are shown in **figure 2**. This data revealed that despite the similarity in size and geometry of the LiO_6 octahedral site and TaO_6 octahedral site, there is no disordering between Ta and Li on these sites.

Table 1. Structure Parameters and Atomic Positions of La_2LiTaO_6

Structure Parameters				
Formula weight	561.70 g			
Crystal system	monoclinic			
Space group	*P* 1 21/n 1 (no. 14)			
Unit cell dimensions	*a* = 5.6182(3) Å			
	b = 5.7663(3) Å			
	c = 7.9487(4) Å			
	β = 90.31(0) °			
Cell volume	257.50(3) $Å^3$			
Z	2			
Density, calculated	7.244 g/cm^3			
Atomic Positions				
Atom	***x***	***y***	**z**	**U_{iso} (×100)**
La	0.4939(7)	0.0471(4)	0.2528(5)	1.40(5)
Li	0		0	
Ta	0.5		0.5	
O1	0.2136(8)	0.3144(8)	0.0449(7)	1.30(4)
O2	0.5971(7)	0.4726(6)	0.2396(5)	1.30(4)
O3	0.3160(8)	0.7871(8)	0.0501(6)	1.30(4)

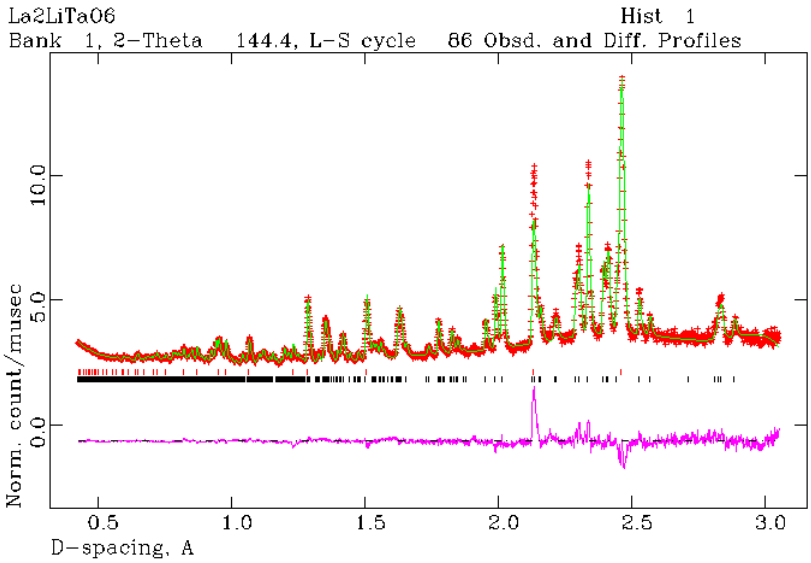

Figure 2.
Neutron scattering data for La_2LiTaO_6. Orange is the experimental spectrum, green is the calculated spectrum, pink is the difference spectrum (between observed and calculated) and the black vertical marks are the calculated peak positions.

Views of this structure can be seen in **figure 3**. Similar to the structure of LiLaTa-garnet, the lanthanum is 8-coordinate in this structure, but more distorted with La-O bond lengths ranging from 2.3-2.8 Å. The Li and Ta are both octahedral. The Li-O distances are 2.1-2.2 Å, and the Ta-O distances are shorter; 1.96-2.20 Å. Also in this structure, the La-site is ideal for Eu-doping and the Li and Ta sites are the appropriate size for Mn. **Figure 3a** emphasizes the octahedral Li-site. Unlike the garnet phase in which Li-sites are connected and allow site-hopping, this Li-site is completely isolated from other Li-sites. Rather it shares three faces with La-polyhedra. The structure view in **figure 3b** emphasizes the Ta-site. The TaO_6 octahedron shares three edges with La-polyhedra, and three corners with LiO_6 octahedra. These two octahedral sites are distinctly different in their neighboring polyhedra, which may influence the luminescence properties. Therefore it will be very interesting to determine if the Mn-dopant resides on the Li-site, the Ta-site or perhaps both; in this phase and other phases that will be studied in the future (see Conclusions and Future Work).

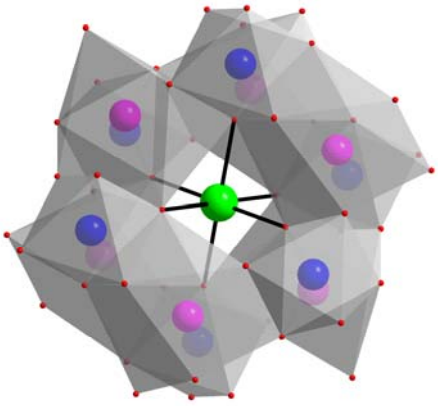

Figure 3a.
First view of LiLaTa-perovskite, focused on the octahedral lithium site (green sphere). Pink spheres are La, blue spheres are Ta.

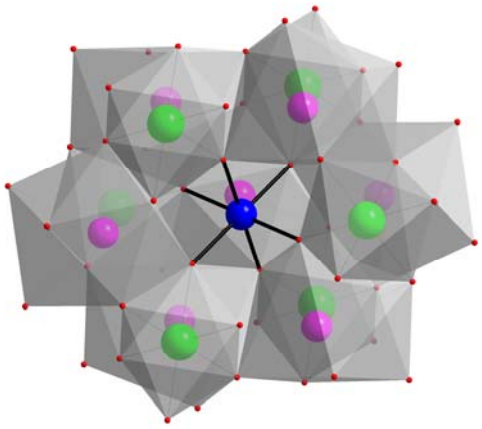

Figure 3b.
Second view of LiLaTa-perovskite, focused on the octahedral tantalum site (blue sphere).

2.2 Different methods of Synthesis and Doping

In this study, LiLaTa-garnet was always synthesized by solid-state methods (see experimental), and the Eu was included in the framework by replacement of the La by Eu in the synthesis mixture. Up to 30% of the La could be replaced by Eu and still retain the garnet structure. The LiLaTa-perovskite could likewise be synthesized directly in the solid-state, or it could be formed by conversion from LiLaTa-garnet. In this process, the lithium is partially exchanged for protons (acidification) and then heated above 850 ˚C to volatilize H_2O (see experimental for details).(**10**) However the phase that forms has a formula that differs from $LiTaLa_2O_6$. The steps of conversion are as follows:

$$Li_5La_3Ta_2O_{12} \rightarrow pH\text{-}2 \rightarrow LiH_4La_3Ta_2O_{12} + 4LiOH \qquad (1)$$

$$LiH_4La_3Ta_2O_{12} \rightarrow 1100\ ^{\circ}C \rightarrow 1.5\ Li_{0.667}Ta_{1.333}La_2O_{6.8} + 2H_2O \qquad (2)$$

At this point of the research, these equations are only approximations. The amount of Li exchanged for protons is determined by thermogravimetric analysis of the proton-exchanged LiLaTa-garnet. **Figure 4** shows that 20% of the Li is removed by a neutral aqueous exchange, and 80% of the Li is removed by an aqueous exchange at pH-2. In both cases, an exothermic phase change in the DTA (differential thermal analysis) curve is observed at 825 °C. However, given that the La:Ta ratio of the garnet is 1.5:1 and for the perovskite is 2:1, there needs to be excess Ta in the perovskite phase, when formed by conversion of the garnet phase. This requires both slightly reduced Li and slightly excess oxygen for both charge-balance and occupancy requirements. Both are possible, given the excellent size-match of octahedral Li and Ta. Structural and compositional characterization of this derivative of LiLaTa-perovskite is currently underway. While the Eu can only be introduced via the solid-state reaction, we have other options for incorporating Mn into the framework. It can either be introduced by the solid-state synthesis or by ion exchange into the initially acid-exchanged garnet phase (see experimental section), and this is discussed further in the following section.

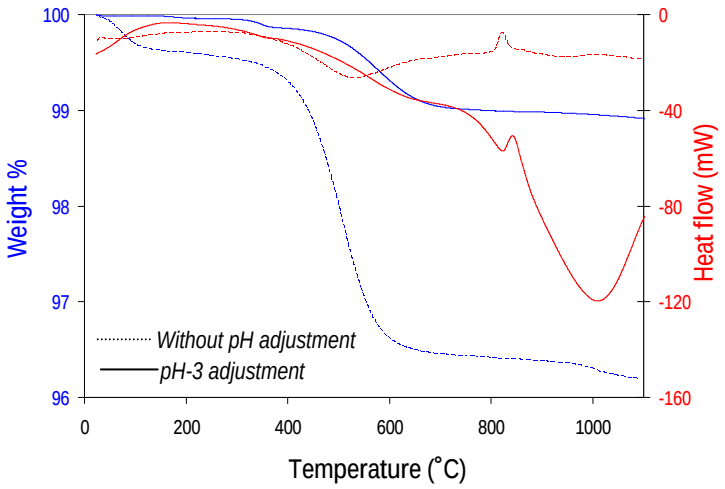

Figure 4.
TGA-DTA of $H^+ \rightarrow Li^+$ exchanged LiLaTa-garnet. Solid line is exchange at neutral pH, dashed lines is exchange at pH-2.

Attempts to generate enough lithium and oxygen vacancies in LiLaTa-garnet to observe self-activated luminescence were not successful. This was attempted by several methods including extensive heating, acid-exchange followed by heating, and doping with tetrahedral anions such as silicate and phosphate. In some cases, a weak glow under UV-light was observed that ranged from red to purple in color. However, it was not strong enough to perform meaningful measurements. We also attempted to produce visible emission on related LiLaTa-perovskite and Li_3TaO_4; but again, only weak emission was observed. Therefore the discussion in the following section is on the Eu-doped and Mn-doped lithium lanthanum tantalate materials and their adsorption and emission characteristics. Several characteristics were of interest; those specifically related to the performance of the red phosphor in a blue-pumped LED. In particular, the line-width of the blue adsorption peak should be broad to increase the overlap between the blue LED emission and the blue-adsorbing phosphor, and the quantum yield (ratio of light emitted to light adsorbed) should be high. Of previous pyrochlore tantalates ($KLnTa_2O_7$:Eu; Ln=Lu,Y,Gd and $LaTaO_4$) measured, the blue adsorption peak is generally centered at 464 nm **(1,3)**.

2.3 Characterization of Doped Lithium Lanthanum Tantalate

2.3.1 Eu-doped LiLaTa phases

Eu-doped LiLaTa-garnet was synthesized by solid-state methods**:** up to 30% Eu doping was achieved before impurity phases formed. The Eu-doped LiLaTa-garnet can also be acid-exchanged to partially remove lithium and then converted LiLaTa-perovskite, as described above. For the above-mentioned rare-earth tantalate phases, the adsorption peak increases in broadness in the following order: RE = La < Y < Lu < Gd. The Gd tantalate had the broadest 464 nm adsorption peak with FWHM~15 nm, and the La tantalate had the narrowest adsorption peak, FWHM around 5nm. While also located at 464 nm, the adsorption peaks for LiLaTa-garnet and perovskite (regardless the synthesis method) were not any broader; with FWHM~5

nm—see **figure 5**. Furthermore, the Eu-doped garnet and perovskite phases did not provide better quantum yields (QY) than the previously characterized rare-earth tantalates, with a maximum QY of 23%; see **Table 2**.

Table 2. Comparison of QY of Rare-Earth Tantalates doped with Eu or Mn

RE tantalate	Max QY	Eu doping (%)	Mn doping (%)
$KGdTa_2O_7$	76	17.5	
$KLuTa_2O_7$	65	10	
$KYTa_2O_7$	65	10	
$LaTaO_4$	55	10	
LiLaTa-garnet	23	10	
LiLaTa-perovskite	5.6	10	
LiLaTa-perovskite	17	20	
LiLaTa-garnet		NYD*	trace
LiLaTa-perovskite		30	trace

**NYD=not yet determined*

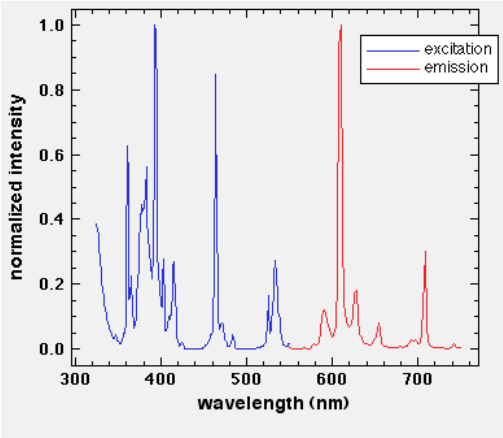

Figure 5a.
Excitation and emission spectra of 10%Eu-substituted LiLaTa-garnet.

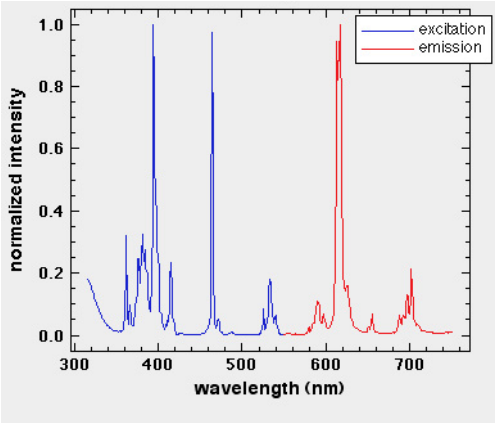

Figure 5b.
Excitation and emission spectra of 10%Eu-substituted LiLaTa-perovskite, derived from the related garnet phase.

Unfortunately, the Eu-doped LiLaTa garnets and perovskites did not yield better phosphor properties, neither via broadening the adsorption peak nor increasing the quantum yield. Therefore we will not likely pursue these any further.

2.3.2 Mn-doped LiLaTa Phases

The Mn-doped LiLaTa-garnet could be synthesized either by incorporating the Mn directly in the solid-state mixture, or by introducing it via ion-exchange. The ion exchange process was either an acid exchange of the garnet followed by a Mn-exchange, or a simultaneous introduction of acid plus Mn. Although the Mn was introduced as divalent (Mn^{2+}), the red emission the red emission is indicative of oxidation to tetravalent (Mn^{4+}). By the solid-state incorporation of Mn, we initially attempted 2% doping of Mn for Ta, This route was not ideal, in that even at this low

doping level, manganate impurity phases formed. Although some red emission was observed in the mixture of material, it was not strong, in that the Mn tended to concentrate in impurity phases rather than be homogeneously dispersed in the LiLaTa phases. The 0.2% Mn-doped LiLaTa-garnet formed by solid-state synthesis surprisingly had only a very weak red emission. It is clear that the LiLaTa garnet lattice is not a good host for luminescent Mn.

However, when the acidified, Mn-doped LiLaTa-garnet was heated to 1000 ˚C, LiLaTa-perovskite is formed, that glows deep red when observed under a UV-lamp, or a blue LED. The level of Mn-doping responsible for this glow is very low, perhaps less than 1%; in that it is not be detectable via Energy Dispersive Spectroscopy (EDS). We are currently investigating quantification of the Mn-doping, and determining how to optimize the concentration. It could probably best be controlled by the pH of the acid-exchange process. At the current stage of this work, it appears as if the perovskite phase provides an appropriate lattice for Mn-luminescence, but the garnet phase does not. Therefore we also attempted direct solid-state synthesis of the perovskite phase with incorporation of 2% Mn. Similar to the synthesis of the garnet-phase, this route proved difficult in producing a pure-phase material with red luminescence from Mn-doping. Again the doping level is likely too high, and manganate phases form, depleting the LiLaTa-perovskite of virtually all of the Mn. On the other hand, solid-state synthesis of the LiLaTa-perovskite with only 0.2% Mn doping has a strong deep-red emission. Complete characterization and comparison of the luminescence characteristics of the two types of Mn-doped LiLaTa-perovskite is underway, in order to optimize these materials.

Figure 6 shows the adsorption and emission spectra of Mn-doped LiLaTa-perovskite (left) and Mn,Eu-codoped LiLaTa-perovskite (right). The Eu has typical sharp adsorption and emission peaks, in that the f-f orbital transitions are minimally affected by geometry of the coordination site, bond lengths or linking to neighboring polyhedra. The Mn adsorption and emission on the other hand are very broad. While the excitation peak of Eu is located at around 464 nm and is less than 5 nm wide, the excitation peak for Mn spans 440 to 540 nm, and is obviously much broader. However it peaks between 480-500 nm which is a little longer wavelength than a typical blue LED. The emission peak of Mn is a deeper red (700 nm) than that of Eu (~ 620 nm). The deep red is similar to that of Eu^{2+}-doped oxynitridosilicates, the commercial phosphor used in Lumileds Lighting, LLC LEDs. (**13**) In the Mn,Eu-codoped LiLaTa-perovskite, the Eu is ~10% substituted for La while the Mn is <1% substituted for Ta/Li, meaning there is greater than 10× more Eu than Mn in the lattice. Yet, it is obvious by **figure 6** that the adsorption and emission from the Mn is much higher intensity than that of the Eu. This finding suggests these Mn-doped materials are definitely worth further investigation as phosphors for the blue LED for solid-state lighting. Particularly of interest is the very broad blue adsorption peak, in that it increases chance for overlap with the blue LED emission, even with shifts in the blue emission due to common manufacturing inconsistencies. The narrow adsorption peak of the Eu-doped perovskite is a distinct drawback common to almost all Eu-doped materials, in that it cannot adsorb enough light to efficiently down-convert the intense blue light of the GaAlN LED. Additionally, the Mn-dopant has a strong broad adsorption peak in the UV; from 300-400 nm, so it can also be efficiently excited by UV and can thus be used more generally in other applications.

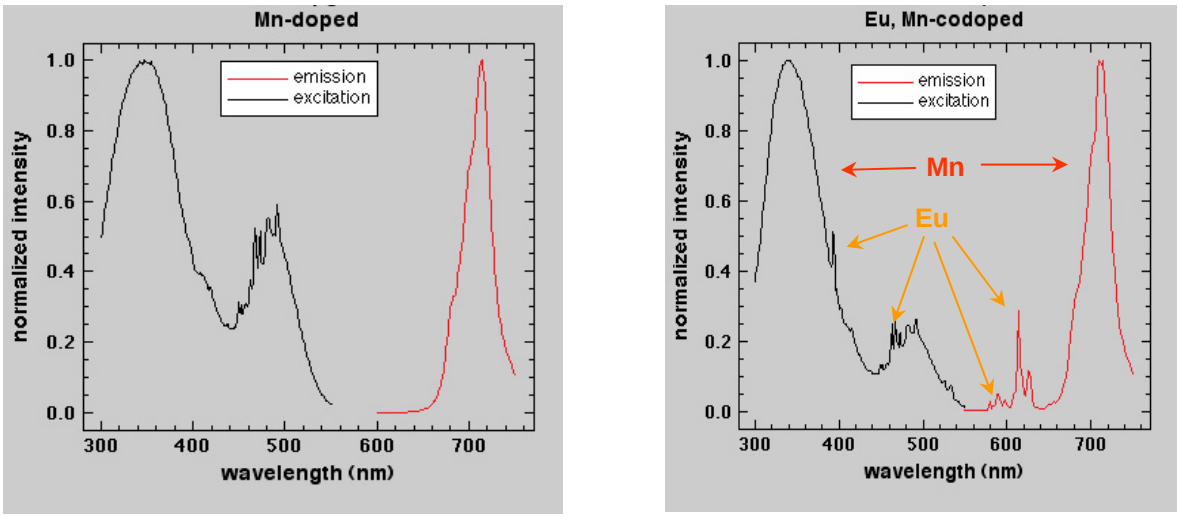

Figure 6.
Left—Mn-doped LiLaTa-perovskite. Right—Eu, Mn-codoped LiLaTa-perovskite. On the right, the adsorption and emission peaks labeled in orange are from Eu, and the adsorption and emission peaks labeled in red are from Mn.

3. EXPERIMENTAL

3.1 Synthesis of LiLaTa-phases

Our synthesis of the garnet phases was adapted from the previously reported procedure.(**14**) In a typical reaction, 10 grams of lanthanum nitrate hexahydrate (23 mmol $La(NO_3)_3 \cdot 6H_2O$), 3.89 grams Ta_2O_5 and 2 grams $LiOH \cdot H_2O$ (38.3 mmol) are placed in a 60 ml plastic tube with ~ 30 YSZ milling beads and 20 ml isopropanol. The tube is capped tightly and sealed with electrical tape and mixed on a Turbula® System Schatz WAB (Basel, Switzerland) for 20-60 minutes. The resulting slurry is thick and homogeneous, resembling white paint. The slurry is poured into a ceramic crucible, filtering out the shaking beads. The crucible is then placed in a vacuum oven at ~ 40 ˚C overnight. Note: at this step, the slurry never completely dries, probably due to the hygroscopic nature of the lanthanum nitrate. The crucible containing the precursor mixture is then heated in a box furnace at 700 ˚C for 6-12 hours. This step results in decomposition of the nitrate salt. In the second processing step, the powder is then re-mixed with ~0.4 g $LiOH \cdot H_2O$ and placed in a 900 ˚C furnace overnight. At this step, the powder product is nearly pure garnet phase, as determined by powder X-ray diffraction, and is white in color.

3.2 Conversion of LiLaTa-garnet to LiLaTa-perovskite

When a powder sample of $Li_5La_3Ta_2O_{12}$ is placed in water in a beaker and stirred, the pH rises to around 10-11 (depending on the concentration of the powder). This is due to exchange of H^+ from the aqueous media, which displaces Li^+ from the garnet lattice. To this slurry, we add drop wise a 1 M HNO_3 solution, while stirring at room temperature and monitoring the pH. When the pH reaches 2.0, the solution is left stirring for another hour. The pH rises to ~3.5 during this time. The $H^+ \rightarrow Li^+$ exchanged garnet powder is then re-collected by vacuum filtration. This powder is then heated to 900 °C or above, in that the conversion to the perovskite phase takes place at 850 °C. Usually we heat at 1000 or 1100 °C for ~30 minutes.

3.3 Solid-state Mn and Eu Doping

For the Eu-doped LiLaTa-garnet, the amount of lanthanum nitrate is reduced and substituted with europium nitrate so the total amount of rare-earth is 23 millimoles. For instance; for 10% Eu-substituted LiLaTa-garnet, 23 mmol $La(NO_3)_3 \cdot 6H_2O$ (10 grams) and 2.57 mmol $Eu(NO_3)_3 \cdot 6H_2O$ (1.15 grams) is utilized. For 0.2-2% Mn-doped samples, we presume the Mn substitutes on either the Ta-site or the Li-site. However, we did not reduce the amount of Ta_2O_5 or LiOH in the reaction to accommodate the Mn, since it is a fairly negligible amount. Mn is introduced to the solid-state reaction mixture as $Mn(NO_3)_2 \cdot xH_2O$.

3.3 Mn-doping by Ion-exchange

This is achieved either simultaneously with the $H^+ \rightarrow Li^+$ exchange (see 3.2) or as a Mn exchange step, following the acid-exchange. In the former, we utilize a 1 M HNO_3/0.01M Mn(II) solution. In the latter case, after the $H^+ \rightarrow Li^+$ exchanged garnet phase is isolated, it is then stirred in a 0.01 M Mn(II) solution for 1 hour, then recollected via vacuum filtration and washing.

3.4 Structure Determination of LiLaTa-perovskite

Time-of-flight neutron diffraction data were collected at 100 K, 200 K and 300 K using an aluminum can attached to a displex at the High-Pressure Preferred Orientation (HiPPO) beamline of the Los Alamos Neutron Scattering Center (LANSCE). The neutron data were analyzed using the Rietveld method with the General Structure Analysis System (GSAS) program.

4. CONCLUSIONS AND FUTURE WORK

This scoping project on developing new red phosphors, for solid-state lighting applications in particular, has produced many promising preliminary results that require further and more thorough examination. While Eu-doped LiLaTa phases were not better than previously reported phases, the Mn-doped LiLaTa phases warrant further investigation. In particular, the significant adsorption of blue light via the Mn-doped LiLaTa-perovskite provides a promising material for blue LED down-convertors for solid-state lighting. Additionally, this LiLaTa-perovskite phosphor is formed optimally by the unique ion-exchange process not previously reported in the scientific literature. Further work to optimize this material and related materials includes to following:

- Structural characterization of the LiLaTa-perovskite obtained from acidification and heating of LiLaTa-garnet to determine how they differ. Compare luminescence characteristics of Mn-doped LiLaTa-perovskite from direct synthesis and that obtained from conversion from the garnet phase.

- Complete characterization of the Mn-doped phases to determine the optimal concentration of the Mn, and the site of doping (Li or Ta or both).

- Synthesis and optical characterization of analogous Mn-doped LiLaNb phases

- Determine the generality of the ion-exchange doping process of the LiLaTa garnet phases. i.e. can other phosphor dopants that are octahedrally coordinated be introduced in a similar manner (i.e. $Cu^{1+/2+}$, Cr^{3+})?

- Finally, we will investigate lithium tantalate phases as novel red phosphors; by ion-exchange and by direct incorporation of the dopant via synthesis (both soft-chemical synthesis and solid-state synthesis). This is extremely important to develop rare-earth free phases given the potential limited availability of these resources on the global market in the near future.

5. REFERENCES

1. May Nyman, Mark A. Rodriguez, L.E. Shea-Rohwer, James E. Martin, Paula P. Provencio, *Highly Versatile Rare Earth Tantalate Pyrochlore Nanophosphors,* Journal of the American Chemical Society, 131(33), 11652, **2009**.

2. L.H. Brixner and H.Y. Chen, *On the Structural and Luminescent Properties of the M'LnTaO$_4$ Rare-earth Tantalates*, Journal of the Electrochemical Society, 130(12), 2435-2443, **1983**.

3. May Nyman, Mark A. Rodriguez, Lauren E. S. Rohwer, James E. Martin, Mollie Waller, Frank E. Osterloh, *Unique LaTaO$_4$ Polymorph for Multiple Energy Applications*, Chemistry of Materials, 21(19), 4731-4737, **2009**.

4. Bo Liu, Kun Han, Xiaolin Liu, Mu Gu, Shiming Huang, Chen Ni, Zeming Qi, Guobin Zhang, *Luminescent properties of GdTaO$_4$ and GdTaO$_4$: Eu^{3+} under VUV-UV excitation*, Solid State Communications, 144(10-11), 484-487, **2007**.

5. Edmund J. Cussen, *The structure of lithium garnets: cation disorder and clustering in a new family of fast Li$^+$ conductors*, Chemical Communications, 4, 412-413, **2006**.

6. Junji Awaka, Norihito Kijima, Yasuhiko Takahashi, Hiroshi Hayakawa, Junji Akimoto, *Synthesis and crystallographic studies of garnet-related lithium-ion conductors Li$_6$CaLa$_2$Ta$_2$O$_{12}$ and Li$_6$BaLa$_2$Ta$_2$O$_{12}$*, Solid State Ionics, 180, (6-8), 602-606, **2009**.

7. R. Murugan, V. Thangadurai, W. Weppner, *Effect of lithium ion content on the lithium ion conductivity of the garnet-like structure Li$_{5+x}$BaLa$_2$Ta$_2$O$_{11.5+0.5x}$ (x = 0-2)*, Applied Physics A-Materials Science & Processing, 91(4), 615-620, **2008**.

8. Michael P. O'Callaghan, Edmund J. Cussen, *Lithium dimer formation in the Li-conducting garnets Li$_{5+x}$Ba$_x$La$_{3-x}$Ta$_2$O$_{12}$ (0 < x <= 1.6)*, Chemical Communications, 20, 2048-2050, **2007**.

9. G. Blasse, M.J.J. Lammers, H.C.G. Verhaar, L.H. Brixner, C.C. Torardi, *The Luminescence of Trigonal Bipyramidal NbO$_5^{5-}$ and TaO$_5^{5-}$ and a Comparison with other Niobates and Tantalates*, Journal of Solid-State Chemistry, 60(2), 258-261, **1985**.

10. May Nyman, Todd M. Alam, Sarah K. McIntyre, Grant C. Bleier, David Ingersoll, *Alternative Approach to Increasing Li Mobility in Li-La-Nb/Ta Garnet Electrolytes*, Chemistry of Materials, 22(19), 5401-5410, **2010**.

11. K. Hayashi, H. Noguchi and S. Fujiwara, *New Phases in La$_2$O$_3$-Li$_2$O-Ta$_2$O$_5$ System*, Mat. Res. Bull. 21, 289-293, **1986**.

12. R.C. Currie, J.F. Vente, E. Frikkee, D.J.W. Ijdo, *The Structure and Magnetic Properties of La_2MIrO_6 with M=Mg, Co, Ni, and Zn*, Journal of Solid-State Chemistry, 116, 199-204, **1995**.

13. R. Mueller-Mach, G. Mueller, M.R. Krames, H.A. Hoppe, F. Stadler, W. Schnick, T. Juestel, P. Schmidt, *Highly Efficient All-Nitride Phosphor-Converted White Light Emitting Diode*, Physica Status Solidi A—Applications and Materials Science, 202(9), 1727-1732, **2005**.

14. V. Thangadurai, S. Adams, W. Weppner, *Crystal Structure Revision and Identification of Li^+-Ion Migration Pathways in the Garnet-like $Li_5La_3M_2O_{12}$ (M=Nb,Ta) Oxides*, Chemistry of Materials, 16(16), 2998-3006, **2004**.

DISTRIBUTION

1	MS0359	D. Chavez, LDRD Office	1911
1	MS0899	Technical Library	9536 (electronic copy)


Sandia National Laboratories